



47-fs Kerr-lens mode-locked Cr:ZnSe laser with high spectral purity

YUCHEN WANG,^{1,2} TONEY T. FERNANDEZ,¹ NICOLA COLUCCELLI,^{1,2}
ALESSIO GAMBETTA,^{1,2} PAOLO LAPORTA,^{1,2} AND GIANLUCA
GALZERANO^{1,2,*}

¹Istituto di Fotonica e Nanotecnologie - Consiglio Nazionale delle Ricerche, Piazza Leonardo da Vinci 32, 20133 Milano, Italy

²Dipartimento di Fisica - Politecnico di Milano, Piazza Leonardo da Vinci 32, 20133 Milano, Italy

*gianluca.galzerano@polimi.it

Abstract: We report on a room-temperature Kerr-lens mode-locked Cr:ZnSe femtosecond laser operating at around 2.4 μm emission wavelength. Self-starting nearly transform-limited pulse trains with a minimum duration of 47 fs, corresponding to six optical cycles, and average output power of 0.25 W are obtained with repetition frequencies in the range from 140 to 300 MHz. The femtosecond pulse train is characterized by high-spectral purity and low time jitter.

© 2017 Optical Society of America

OCIS codes: (140.7090) Ultrafast lasers; (140.3070) Infrared and far-infrared lasers; (160.6990) Transition-metal-doped materials.

References and links

1. S. Mirov, V. Fedorov, D. Martyshkin, I. Moskalev, M. Mirov, and S. Vasilyev, "Progress in Mid-IR lasers based on Cr and Fe-Doped II-VI chalcogenides," *IEEE J. Sel. Top. Quantum Electron.* **21**, 292–310 (2015).
2. I. T. Sorokina and E. Sorokin, "Femtosecond Cr²⁺-based lasers," *IEEE J. Sel. Top. Quantum Electron.* **21**, 1601519 (2015).
3. S. Vasilyev, I. Moskalev, M. Mirov, V. Smolski, S. Mirov, and V. Gapontsev, "Ultrafast middle-IR lasers and amplifiers based on polycrystalline Cr:ZnS and Cr:ZnSe," *Opt. Mater. Express* **7**, 2636–2650 (2017).
4. I. T. Sorokina, E. Sorokin, and T. Carrig, "Femtosecond pulse generation from a SESAM mode-locked Cr:ZnSe laser," in *Proceedings of the Conference on Lasers and Electro-Optics/Quantum Electronics Laser Science Long Beach, CA, USA, 2006*, Paper CMQ2.
5. E. Sorokin and I. T. Sorokina, "Ultrashort-pulsed Kerr-lens modelocked Cr:ZnSe laser," in *Proceedings of CLEO/Europe 2009, Munich, Germany, June 15–19, 2009*, p. CF1.3.
6. M. N. Cizmeciyan, H. Cankaya, A. Kurt, and A. Sennaroglu, "Kerr-lens mode-locked femtosecond Cr²⁺:ZnSe laser at 2420 nm," *Opt. Lett.* **34**, 3056–3058 (2009).
7. E. Slobodchikov and P. F. Moulton, "1-GW-peak-power, Cr:ZnSe laser," in *Proceedings of the Conference on Lasers and Electro-Optics*, Baltimore, MD, USA, 2011.
8. M. N. Cizmeciyan, H. Cankaya, A. Kurt, and A. Sennaroglu, "Operation of femtosecond Kerr-lens mode-locked Cr:ZnSe lasers with different dispersion compensation methods," *Appl. Phys. B* **106**, 887–892 (2012).
9. S. Vasilyev, M. Mirov, and V. Gapontsev, "Kerr-lens mode-locked femtosecond polycrystalline Cr²⁺:ZnS and Cr²⁺:ZnSe lasers," *Opt. Express* **22**, 5118–5123 (2014).
10. A. Schliesser, N. Picqué, and T. W. Hänsch, "Mid-infrared frequency combs," *Nat. Photonics* **6**, 440–449 (2012).
11. S. Vasilyev, I. Moskalev, M. Mirov, S. Mirov, and V. Gapontsev, "Three optical cycle mid-IR Kerr-lens mode-locked polycrystalline Cr²⁺:ZnS laser," *Opt. Lett.* **40**, 5054–5057 (2015).
12. S. Vasilyev, I. Moskalev, M. Mirov, S. Mirov, and V. Gapontsev, "Multi-Watt mid-IR femtosecond polycrystalline Cr²⁺:ZnS and Cr²⁺:ZnSe laser amplifiers with the spectrum spanning 2.0–2.6 μm ," *Opt. Express* **24**, 1616–1623 (2016).
13. R. Szipöcs, C. Spielmann, F. Krausz, and K. Ferencz, "Chirped multilayer coatings for broadband dispersion control in femtosecond lasers," *Opt. Lett.* **19**, 201–203, (1994).
14. M. Baudrier-Raybaut, R. Häidar, P. Kupecek, P. Lemasson, and E. Rosencher, "Random quasi-phase-matching in bulk polycrystalline isotropic nonlinear materials," *Nature* **432**, 374–376 (2004).
15. E. Sorokin and I. T. Sorokina, "Femtosecond Operation and Random Quasi-Phase-Matched Self-Doubling of Ceramic Cr:ZnSe Laser," in *Proceedings of the Conference on Lasers and Electro-Optics 2010, OSA Technical Digest (CD) (Optical Society of America, 2010)*, paper CTuGG2.
16. D. von der Linde, "Characterization of the noise in continuously operating mode-locked lasers," *Appl. Phys. B: Photophys. Laser Chem.* **39**, 201–217 (1986).

17. C. C. Harb, T. C. Ralph, E. H. Huntington, D. E. McClelland, and H. A. Bachor, "Intensity-noise dependence of Nd:YAG lasers on their diode-laser pump source," *J. Opt. Soc. Am. B* **14**, 2936 (1997).

1. Introduction

Femtosecond laser sources operating in the middle-infrared (mid-IR) spectral range with high-repetition rates are of utmost interest for a variety of applications ranging from ultrafast spectroscopy, high-resolution and broadband spectroscopy, quantum optics, frequency metrology and synthesis of mid-IR optical frequency combs. In the last years a great effort has been devoted to develop ultrashort laser pulse trains in the mid-IR at around $3\ \mu\text{m}$ and beyond, where inorganic and organic molecules show their strongest absorption features associated with fundamental roto-vibrational transitions. Among the different laser media emitting in the spectral region around $3\ \mu\text{m}$, bulk lasers based on Cr^{2+} -doped binary chalcogenide crystals (such as ZnSe, ZnS, and CdSe), with gain bandwidths up to 50% of the central wavelength, represent the mid-IR analog of titanium-doped sapphire laser in terms of strong and ultra-broad emission bands in the spectral region from 2.1 to $3.1\ \mu\text{m}$ [1]. In particular, passive mode-locking of Cr-doped chalcogenide lasers [2, 3] represents an ideal alternative to generate high-repetition rate femtosecond mid-IR pulses as compared to the complex ultrafast sources based on down-conversion of near-IR lasers in optical parametric oscillators and difference-frequency generation setups. Since the first demonstration of femtosecond Cr:ZnSe lasers [4], Kerr-lens mode locking (KLM) in polycrystalline Cr:ZnSe led to significant improvements in the output parameters of ultrafast mid-IR lasers in terms of average power, pulse energy, and pulse duration [5–9]. Concerning the demanding applications related to the use of optical-frequency combs based on mid-IR mode-locked femtosecond lasers [10], spectral purity and time jitter stability properties are particularly relevant. However, these properties have not been fully investigated yet in femtosecond lasers based on Cr-doped chalcogenide crystals.

In this paper, we demonstrate a 47-fs KLM Cr:ZnSe laser at $2.4\ \mu\text{m}$, based on chirped-mirror dispersion-controlled resonator, delivering nearly transform-limited pulse trains at 300 MHz repetition rate with average output power of 250 mW. In particular, the laser has been fully characterized in terms of pulse intensity noise and repetition frequency stability. The integrated phase noise from 100 Hz to 10 MHz is 1 mrad, corresponding to a relative time jitter of 10^{-4} . Although the minimum duration of 30 fs, recently obtained with a KLM Cr:ZnS laser [11, 12] has not been reached, the measured 47-fs pulsewidth turns out to be, to the best authors' knowledge, the shortest so far reported in the literature for a Kerr-lens mode-locking in polycrystalline Cr:ZnSe. The excellent performance characterizing this femtosecond source opens the way to implement a novel-type of mid-IR optical frequency comb synthesizer, based on high-repetition rate KLM Cr:ZnSe laser, covering the near and mid-IR fingerprint spectral region from 1 to $4\ \mu\text{m}$.

2. KLM Cr:ZnSe laser

Figure 1(a) shows the experimental setup of the KLM Cr:ZnSe cavity. The asymmetric x-shape linear resonator consists of six mirrors: two plano-concave high-reflectance chirped mirrors (reflectance $R > 99.5\%$ from 2300 to 2600 nm and nominal GDD=-250 fs²) with a radius of curvature of 50 mm, three plane chirped mirrors (same coating of the plano-concave ones), and a wedged 3% output coupler. The 2.8-mm thick Cr:ZnSe polycrystal, with a doping level of 9×10^{18} ions/cm³, is mounted on a copper heat sink kept at constant temperature of 20 °C by a Peltier electric-cooler and a proportional-integrative-derivative temperature controller (1-h temperature stability of 0.1 °C). The Cr:ZnSe crystal is placed in the central section of the laser resonator at Brewster angle between the two spherical mirrors set in a nearly confocal configuration. The spherical mirrors fold the resonator with 15° full angle to compensate for

the astigmatism due to the Brewster-oriented surfaces of the Cr:ZnSe crystal. The outer sections of the resonator are asymmetric with a ratio of 3:5 between the two arms. The total resonator length can be varied between 0.5 to 1.1 m (by changing the positions of both the output coupler and the HR plane terminal mirror), corresponding to pulse repetition rate from 140 to 300 MHz. Fine continuous tuning of the repetition frequency with a relative amount of 5% is obtained by moving the HR plane terminal mirror with a 60 mm travel micrometric stage. The mode spot size inside the gain crystal is $20 \mu\text{m} \times 38 \mu\text{m}$, as calculated by numerical simulations. The pump source is a CW Er:fiber laser (IPG Photonics, ELR-LP-20) with a maximum output power of 20 W and a linearly polarized beam at $1.57 \mu\text{m}$. The pump radiation is focused through the plano-concave chirped mirror ($T = 70\%$ at $1.57 \mu\text{m}$) onto the Cr:ZnSe crystal ($16 \mu\text{m} \times 40 \mu\text{m}$ pump mode spot size), using a plano-convex lens with 50 mm focal length. The single-pass pump power absorption in the crystal (3-mm optical thickness) is $\sim 70\%$. To reduce intracavity absorption and dispersion due to the strong rotovibrational transition of water at around $2.6 \mu\text{m}$, the laser cavity is purged with N_2 in overpressure. The GDD of the resonator is controlled in the $2.2\text{--}2.6 \mu\text{m}$ range using specially designed chirped mirrors (Ultrafast Innovation, GmbH) [13]. Dispersion curves of the gain element (calculated using the standard Sellmeier equation for undoped ZnSe) and of the chirped mirrors (measured by the supplier) are reported in Fig. 1(b). At around $2.4 \mu\text{m}$ the net round-trip intracavity GDD is -700 fs^2 , resulting from $+1260 \text{ fs}^2$ of the active crystal, $+20 \text{ fs}^2$ due to the propagation in N_2 atmosphere, $-220 \times 9 = -1980 \text{ fs}^2$ due

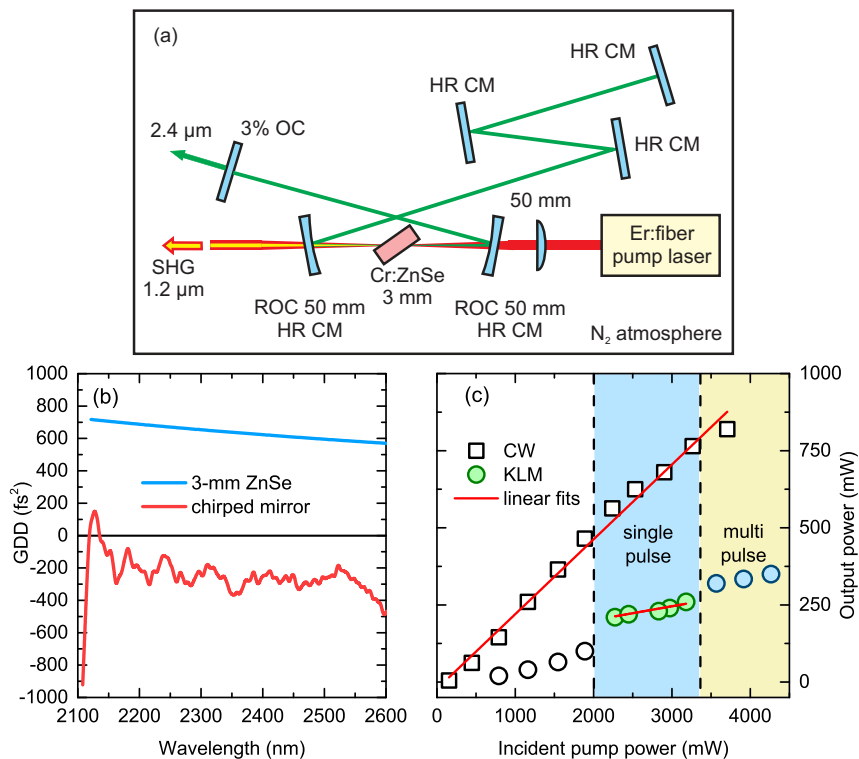


Fig. 1. (a) Astigmatically compensated asymmetric linear cavity configuration. HR CM: high-reflectivity chirped mirror; OC: output coupler; ROC: radius of curvature; SHG: second harmonic generation pulse train. (b) GDD spectra due to the 3-mm thick ZnSe polycrystal and HR CM (single mirror). (c) Output power versus incident pump power in both CW and KLM (300-MHz repetition frequency) regimes.

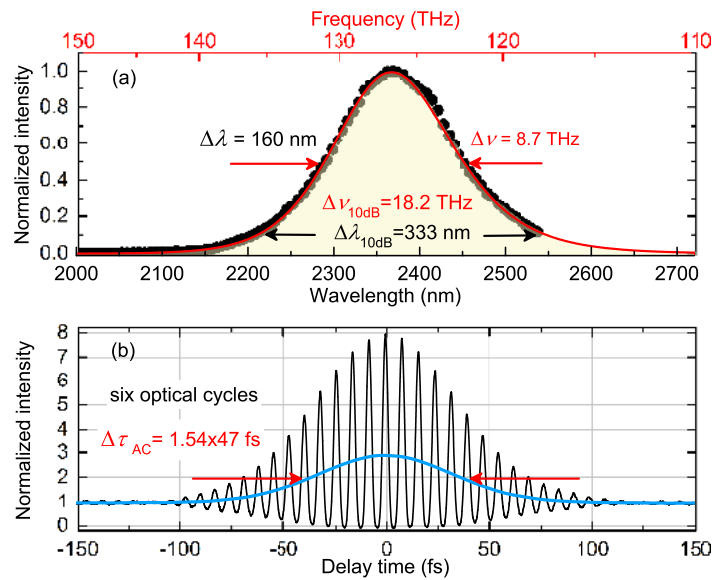


Fig. 2. Spectrum (a) and interferometric autocorrelation (b) of the 150-MHz pulse trains generated by the KLM Cr:ZnSe. The red curve in the spectrum represents the best interpolation for a sech^2 pulse profile leading to a transform-limited pulse width of 37 fs (less than five optical cycles) and a 10 dB bandwidth exceeding 330 nm (18 THz). The blue curve in the autocorrelation corresponds to the intensity autocorrelation profile.

cavity chirped mirrors, excluding the unknown contribution to the GDD arising from the OC (which we estimate in the range from +100 to +200 fs^2). The interplay between the net negative intracavity GDD and the Kerr effect inside the gain crystal leads to a soliton ML regime. To achieve self-starting KLM, the laser resonator is first optimized for maximum CW output power and then both the distance between the curved mirrors and the crystal position are finely adjusted in order to enable the KLM regime, which is initiated by OC translation. Figure 1(c) shows the output power versus the incident pump power in both CW and KLM (300-MHz repetition rate) regimes with 3% output coupling. In the CW regime the Cr:ZnSe laser shows a maximum output power of 0.82 W for an incident pump power of 5.3 W, corresponding to an optical to optical efficiency of 22% with respect to the absorbed pump power. By properly adjusting the cavity alignment, self-starting KLM regime is achieved when the incident pump power is higher than 2.1-W. At 3.2-W pump power a maximum average output power of 0.26 W is obtained for a single-pulse mode-locking. Further increase of the pump power leads to a multi-pulse mode-locking regime with average output powers up to 350 mW.

The spectral bandwidth and the temporal duration of the single-pulse-trains at around $2.4 \mu\text{m}$ are characterized using an extended InGaAs array spectrometer operating in the wavelength range from 0.9 to $2.55 \mu\text{m}$ (OceanOptics, NIRQuest model) and a homemade interferometric autocorrelator, based on two-photon absorption in an InGaAs photodiode (cutoff wavelength $1.7 \mu\text{m}$). Figure 2(a) shows the recorded spectrum at 150-MHz repetition rate together with a fitting curve using a sech^2 pulse shape (red curve). The emission wavelength is centered at 2372 nm (126.5 THz) with a full width at half maximum (FWHM) of 160 nm, corresponding to a bandwidth of 8.7 THz. The corresponding interferometric autocorrelation, characterized by a peak-to-background ratio 8:1, is shown in Fig. 2(b). The retrieved pulse duration is 47 fs (six optical cycles), corresponding to a time-bandwidth product of 0.4 slightly larger than the transform-limited sech^2 product of 0.32, indicating a small residual pulse chirp. Indeed, the

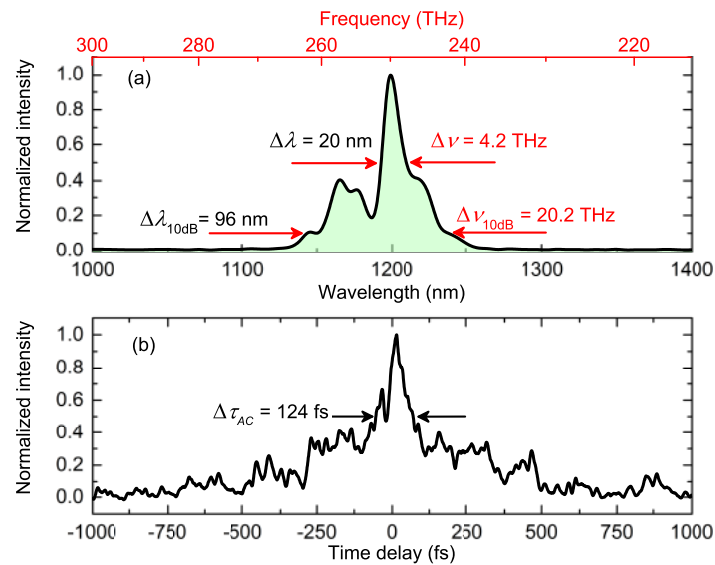


Fig. 3. Spectrum (a) and intensity autocorrelation (b) of the second-harmonic pulse trains generated by the KLM Cr:ZnSe.

generated pulse train reaches the autocorrelation after propagation through a 6.4-mm thick silica substrate of the OC ($GDD = -1210 \text{ fs}^2$ at $2.4 \mu\text{m}$) and, to partially compensate this negative dispersion, it propagates through a 0.4-mm thick Ge plate ($GDD = +780 \text{ fs}^2$ at $2.4 \mu\text{m}$), leading to a residual $GDD = -430 \text{ fs}^2$ which explains the measured time-bandwidth product. Table 1 summarizes the best pulse train characteristics at different repetition frequencies.

Table 1. Pulse train characteristics of KLM Cr:ZnSe laser at different repetition frequencies.

Repetition frequency (MHz)	Average power (W)	Pulse energy (nJ)	Pulse duration (fs)	Pulse bandwidth (nm)	Peak power (kW)
140	0.30	2.1	47	160	44.7
150	0.30	2.0	47	160	42.6
200	0.27	1.4	48	150	29.2
250	0.26	1.0	56	120	17.9
300	0.25	0.8	60	100	13.3

The combined effects of high-intracavity pulse intensity and random quasi-phase matching in the polycrystalline Cr:ZnSe active crystal results in a strong second harmonic generation (SHG) and further three-wave mixing processes, such as third and fourth harmonic generation and parametric sum and difference frequency generation [11, 14, 15]. The strongest SHG signal with an average power of 22 mW was measured at the output of the spherical chirped mirror, as indicated in Fig. 1(a). Additional SHG beams with lower intensities were available at the outputs of the other laser cavity mirrors and can be exploited for alignment purpose and to check the mode-locking regime. The measured SHG emission spectrum and the corresponding intensity autocorrelation at the output of the spherical chirped mirror are shown in Fig. 3(a) and (b), respectively. It should be noted that the SHG spectrum is characterized by a FWHM bandwidth of 20 nm (4.2 THz) and by a 10 dB bandwidth exceeding 90 nm (wider than 20 THz), although the spherical chirped mirror was not optimized for high-transmission at around $1.2 \mu\text{m}$. From the recorded spectrum a transform-limited pulse duration of 40 fs can be inferred. The temporal

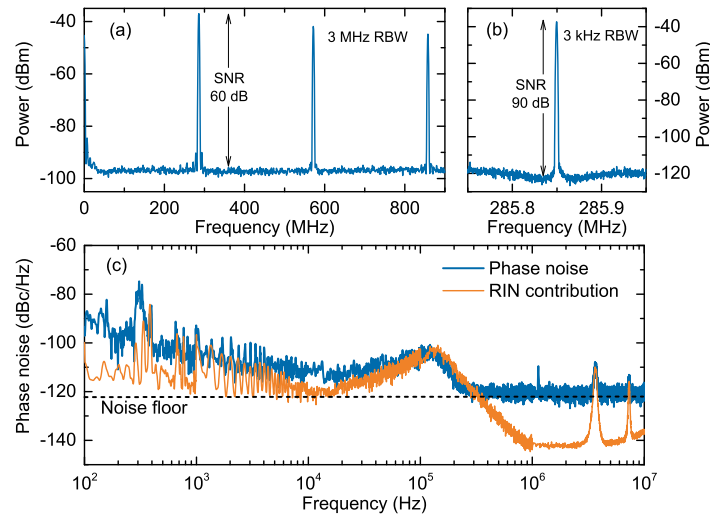


Fig. 4. RF spectrum of the mode-locking pulses measured (a) in a 900-MHz frequency span (3-MHz resolution bandwidth) and (b) at around the fundamental pulse repetition frequency (3-kHz resolution bandwidth). (c) Power spectral density of the phase noise at the fundamental repetition frequency versus the Fourier frequency.

width of the measured autocorrelation trace of the SHG shows a full width at half maximum duration of 124 fs, compatible with a strong group velocity dispersion mainly due to propagation inside the 3-mm thick Cr:ZnSe crystal ($GDD=+1500$ fs²). In principle, proper compensation of the SHG group velocity dispersion may lead to rather short pulse also in the near-IR wavelength range.

3. Spectral purity and frequency stability

To characterize the stability of the KLM laser, first the RF spectrum of the pulse train at the output of the oscillator is measured using a fast InGaAs photodiode (~ 0.5 GHz bandwidth) and an electrical spectrum analyzer (ESA). Figure 4(a) shows the RF spectrum measured in a 900 MHz frequency span with a resolution bandwidth (RBW) of 3 MHz, when the laser is operated at the maximum repetition rate of ~ 300 MHz. The high fundamental carrier-to-noise (SNR) ratio of 60 dB and the absence of any Q-switch sidebands in the RF spectrum proves the excellent pulse-to-pulse stability of the KML regime. The SNR further increases to 90 dB by narrowing the resolution bandwidth to 3 kHz, as shown in Fig. 4(b), indicating a low phase noise and timing jitter of the pulse repetition frequency and period, respectively [16]. To better investigate the time jitter stability, the phase noise power spectral density of the fundamental carrier, $S_\phi(f)$ in [dB_{rad}/Hz], is obtained through the direct measurement of L -script power spectral density, $L(f) = \frac{1}{2}S_\phi(f)$ in [dB_c/Hz], by using the ESA. Figure 4(c) shows the measured $S_\phi(f)$ in the Fourier frequency range from 100 Hz to 10 MHz. It should be noted that for frequencies larger than 300 kHz the measurement is limited by the sensitivity of the ESA (noise floor at -160 dBm/Hz) whereas in the frequency range from 30 to 300 kHz the measured phase noise can not be distinguished from the relative intensity noise (RIN). Phase noise exceeds RIN by few dB only at Fourier frequencies close to the carrier. At low Fourier frequencies a flicker trend can be seen with $S_\phi(f) = 6 \cdot 10^{-8}f^{-1}$ for $0.1 < f < 20$ kHz. The corresponding integrated phase noise is 1 mrad (from 100 Hz to 10 MHz) leading to an absolute time jitter of 530 fs, mainly limited by the RIN. Same results were observed also for lower pulse repetition frequencies.

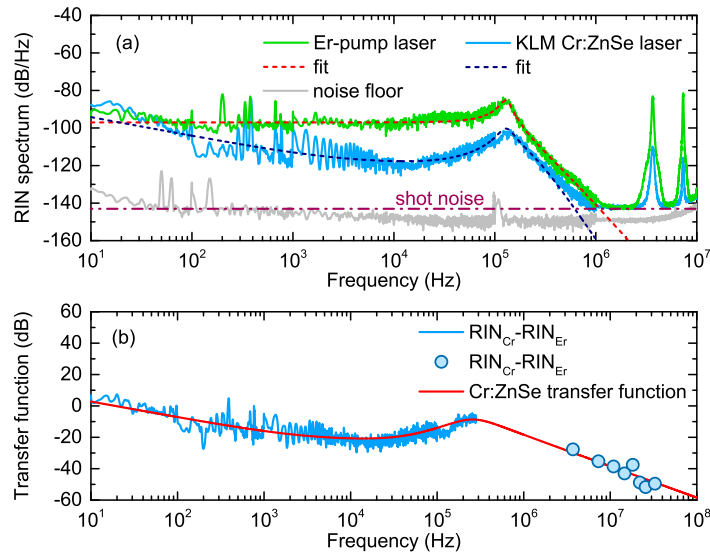


Fig. 5. (a) Relative intensity noise spectral density of both the Er-pump and KLM Cr:ZnSe lasers. Dashed curves represent the theoretical prediction of the RIN spectra. (b) Difference between the RIN spectra of the KLM Cr:ZnSe and Er-fiber pump lasers. Circles represent the difference between the peak values located at the frequency of 3.7 MHz and its harmonics (multilongitudinal mode-beating of the Er-fiber laser). The red line represents the best data interpolation with the transfer function of the KLM Cr:ZnSe system defined by eq. 1 ($K_0=2.5$; $f_z=45$ kHz; $f_0=260$ kHz; $\delta=0.4$).

The RIN of the KLM Cr:ZnSe laser together with that of the pump Er-fiber laser source are shown in Fig. 5(a). RIN measurements have been obtained using a low-noise InGaAs photodetector with 30-MHz bandwidth. The RIN of the KLM Cr:ZnSe laser is always lower than the pump source RIN due to a filtering effect of the KLM Cr:ZnSe system. The RIN of the pump source is characterized by a relaxation resonance at 130 kHz and a low-frequency relative intensity noise of -97 dB/Hz, as sketched in Fig. 5(a) by the dashed red fitting curve, and by several narrow peaks located at the frequency of 3.7 MHz and its harmonics due to multilongitudinal mode-beating of the Er-fiber laser. In particular, the RIN of the KLM Cr:ZnSe laser remains lower than -100 dB/Hz for frequencies larger than 100 Hz, reaching -120 dB/Hz in the range from 2 to 20 kHz; then, due to the pump relaxation oscillation resonance, it increases to -100 dB/Hz at around 130 kHz and, finally, the RIN decreases attaining the quantum-noise limit (-142 dB/Hz) at Fourier frequencies larger than 1 MHz. Over the entire frequency range from 10 Hz to 10 MHz the cumulative standard deviation of the KLM Cr:ZnSe laser intensity amounts to 0.3%, a factor of 3 times lower than the pump laser cumulative standard deviation. To better understand the main contribution to the RIN of KLM Cr:ZnSe, the difference between the two recorded RIN spectra is analyzed as reported in Fig. 5(b). It appears that the experimental results can be well interpolated by the following transfer-function [17]

$$H_{Cr}(f) = K_0 \frac{\left(1 + \frac{f^2}{f_z^2}\right)}{\left[\left(1 - \frac{f^2}{f_0^2}\right)^2 + 2\delta \frac{f^2}{f_0^2}\right]} \quad (1)$$

characterized by a complex-conjugate pair of poles with a relaxation frequency $f_0=260$ kHz and a damping factor $\delta=0.4$, a sensitivity $K_0=2.5$, and a zero located at frequency $f_z=45$ kHz.

According to this transfer function, the KLM Cr:ZnSe RIN can be interpreted as a combination of pump and intracavity losses noises [17]. In particular, intracavity losses noise dominates the Cr:ZnSe RIN at frequencies lower than the relaxation frequency, as evidenced by the presence of the zero in the transfer function, whereas the RIN is limited by the pump noise for frequencies larger than f_0 . By acting on the pump intensity is therefore possible, as in other conventional laser sources, to reduce the RIN using an optoelectronic feedback stabilization loop.

4. Conclusion

In conclusion, Kerr-lens passive mode-locking of a Cr:ZnSe laser operating at $2.4 \mu\text{m}$ with a maximum frequency repetition rate of 300 MHz has been demonstrated in a linear prism-less cavity configuration. Nearly transform-limited pulse-trains with a minimum pulse duration of 47 fs, corresponding to 6 optical cycles, and an average maximum output power of 250 mW have been obtained. The pulse trains are characterized by a very high spectral purity and pulse to pulse stability, mainly limited by the intensity noise of the pump source. In addition, due to random quasi-phase matching in the polycrystalline Cr:ZnSe active crystal, a strong second harmonic generation pulse trains is simultaneously available. Thanks to these unique characteristics the femtosecond Cr:ZnSe laser finds interesting applications in high-resolution molecular spectroscopy, frequency metrology, and in particular for potential generation of high-power mid-IR optical frequency combs.

Funding

Italian Ministry of University and Research (MIUR) and ESFRI Roadmap - Extreme Light Infrastructure (ELI); Cyber-Sort Framework agreement Lombardy Region-CNR (n.19363/RCC).